

Phase transition temperature of SrTiO₃ ultrathin films: An annealing study by ultraviolet Raman spectroscopy

A. B. Shi and W. Z. Shen^{a)}

Laboratory of Condensed Matter Spectroscopy and Opto-Electronic Physics, Department of Physics, Shanghai Jiao Tong University, 1954 Hua Shan Road, Shanghai 200030, China

H. Wu

Department of Applied Physics, Donghua University, 2999 North Ren Min Road, Shanghai 201620, China

(Received 3 June 2007; accepted 27 August 2007; published online 13 September 2007)

The authors present a detailed investigation of paraferroelectric phase transition temperature (T_C) of SrTiO₃ ultrathin films grown by molecular beam epitaxy on Si substrate under various annealing temperatures on the basis of recent understanding of the interfacial layer formation in constant oxygen atmosphere. They show that T_C determined by the ultraviolet Raman spectroscopy is found to enhance linearly with the increasing compressive thermal strain. The present work demonstrates that the “strain engineering” room-temperature ferroelectricity in SrTiO₃ films can also be realized through the rapid controlled annealing, in addition to the substitution of substrates in the literature. © 2007 American Institute of Physics. [DOI: 10.1063/1.2784171]

There is great interest in the perovskite SrTiO₃ (STO) due to a wide variety of applications, including gigabit dynamic random access memories,¹ tunable microwave devices,² a promising substitute for SiO₂ in gate dielectrics or substrate for superconductors,³ etc. However, STO is an incipient ferroelectric in the pure and unstressed form,^{4,5} where large quantum fluctuations suppress the ferroelectricity; and therefore, STO is a quantum paraelectric even at very low temperatures. The enhancement of the STO paraferroelectric phase transition temperature (T_C) is absolutely necessary to make it possible and convenient for the above utilizations. Up to now, there are two ways available to adjust T_C . Traditionally, it is accomplished by chemical or cation substitution such as Ba_xSr_{1-x}TiO₃ (Refs. 6 and 7) or through oxygen isotope exchanges.^{8,9} An alternative way to change T_C is strain, as recent theories and experiments validate the existence of ferroelectricity in STO thin films under strain.^{5,10,11} Strains could be from differences in crystal lattice parameters^{5,11,12} and thermal expansion behavior^{10,13} between the film and the underlying substrate, or from defects formed during film deposition. As a result of strain, the properties of STO thin films have been remarkably changed, offering the opportunity to enhance particular properties of the chosen material, which is called “strain engineering.”¹²

Various substrates, which provide different lattice mismatch strain¹¹ or thermal expansion induced strain,¹⁰ were employed to study the strain dependence of T_C , because the boundary conditions imposed by a substrate profoundly affect ferroelectricity in thin films. Haeni *et al.*⁵ have reported that the DyScO₃ substrate can increase T_C and produce room-temperature (RT) ferroelectricity in STO thin films. Alternately, annealing at high temperatures will not only increase the crystallinity,¹⁴ but also change the boundary conditions (or structure) with the formation of interfacial layers,¹⁵ thus it could probably be a shortcut to adjust T_C through strain from the interfacial layers. In this letter, we focus on the paraferroelectric phase transition temperature of epitaxial ultrathin STO films on Si substrates under various

annealing temperatures (T_A). It should be noted that the annealing process is quite complicated, during which the film and the substrate are unstable next to each other. Fortunately, a number of researchers^{16,17} on the annealing process have shed light on the interfacial structure between epitaxial STO and the underlying silicon.

The studied STO ultrathin (~31 nm) films were grown by molecular beam epitaxy (MBE) on Si substrates in a DCA 450 system. The growth process was monitored by reflection high-energy electron diffraction, where the two-dimensional growth was verified by the observation of persistent intensity oscillations. Due to the large lattice mismatch, the epitaxial STO layers were rotated (normally by 45°) around the Si [001] surface, i.e., the crystallographic orientation of STO (001)||Si (001) and STO [100]||Si [110]. Details of the growth procedures and structural analysis were given elsewhere.^{18,19} The as-grown sample was then cut into four pieces, which were annealed at four different temperatures of 700, 800, 900, and 1000 °C for 2 h under fixed oxygen pressure of 10⁻⁵ mbar. Temperature-dependent Raman measurements were performed on a Jobin Yvon LabRAM HR 800 UV micro-Raman system. Spectra were recorded in the temperature range of 83–303 K in backscattering geometry using 325 nm He–Cd laser line as the excitation source.

Figure 1(a) shows the Raman spectra at 83 K of four STO thin films under different T_A of 700, 800, 900, and 1000 °C. By comparing with the reported results,^{4,18,20,21} we identify the strong peak at 547 cm⁻¹ to the transverse-optical (TO)₄ phonons and the weak peaks at 470 and 790 cm⁻¹ to the longitudinal-optical (LO)₃ and LO₄ phonons, respectively. As marked with “∇,” the high-frequency scattering features around 1290 and 1590 cm⁻¹ are from two-phonon processes of LO₃+TO₃ and 2TO₄, while the weak second-order features can be observed between 600 and 700 cm⁻¹. The very weak Raman structures at 521 and ~1000 cm⁻¹ (labeled with “▼”) are related to the Si substrate.

It is accepted that STO thin films grown on Si belong to displacive phase transition materials, that is, around T_C , the Ti cation moves from its centrosymmetric position towards (001) direction within the perovskite unit cell, leading to a Ti–O bond length distortion interpreted as a ferroelectric

^{a)} Author to whom correspondence should be addressed; electronic mail: wzshen@sjtu.edu.cn

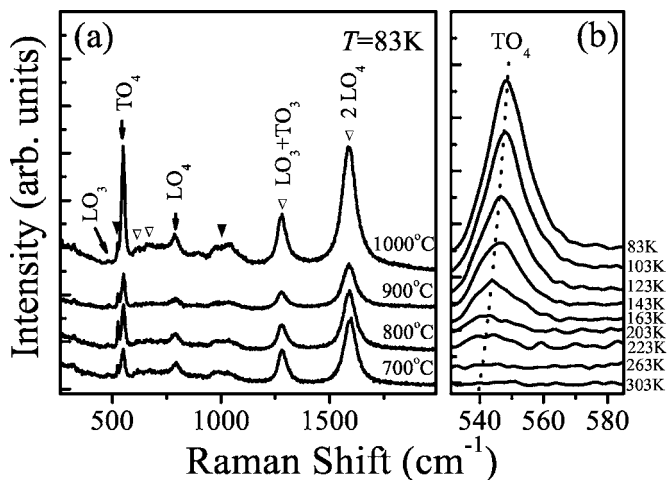


FIG. 1. (a) UV Raman spectra at 83 K of the STO thin films grown by MBE on Si substrate at different T_A of 700, 800, 900, and 1000 °C. Peaks with ∇ are related to the second-order processes, and those with \blacktriangledown to Si substrate. (b) Temperature evolution of TO_4 phonon of the STO thin films under $T_A = 700$ °C. All spectra are plotted on the same scale, offset for clarity.

polarization.²² The soft mode TO_1 , consisting predominantly of Ti–O–Ti bending,²³ has been widely used as an evidence of cubic-tetragonal phase transition.^{10,11} Naturally, TO_4 , caused mainly by Ti–O stretching,²³ can be also taken as a characterization of that paraferroelectric phase transition. In fact, Tenne *et al.*²⁰ have demonstrated recently that UV Raman spectroscopy is an effective technique to measure T_C in ferroelectric ultrathin films and superlattices from the Raman intensities of the hard-mode TO_4 phonons. Figure 1(b) presents the temperature evolution of this TO_4 -mode Raman spectra for the STO film annealed at 700 °C. With the increasing temperature, the intensity of this mode decreases gradually and disappears near RT.

We can accurately determine T_C as the temperature where the first-order Raman intensity becomes zero. Figure 2 displays the temperature dependence of the TO_4 -mode Raman intensity normalized by the thermal population factor (Bose factor) $n+1=[1-\exp(-\hbar\omega/kT)]^{-1}$ (where \hbar is Planck constant divided by 2π , ω is phonon frequency, k is Boltzmann

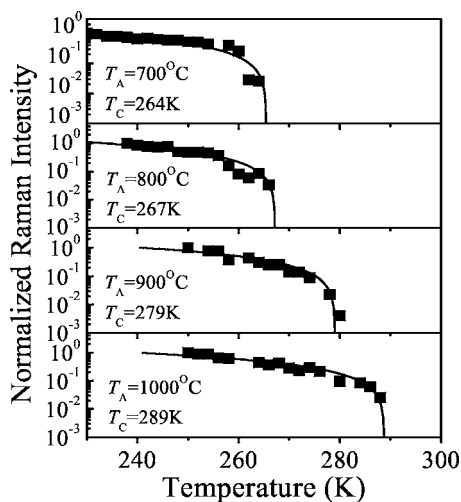


FIG. 2. Temperature dependence of normalized Raman intensities of TO_4 phonons (solid squares) for the four STO thin films with different T_A . The solid curves are fits to the linear temperature dependence.

constant, and T is temperature) and by the Raman intensity at 83 K to correct for the general temperature dependence of Raman intensity. The experimental data demonstrate a linear decay trend with the increase of temperature and the solid curves are linear fits to the results. Taking the intersection of solid curves with the horizontal axes as the transition temperature of the samples, we obtain T_C of 264, 267, 279, and 289 K for the STO films under 700, 800, 900, and 1000 °C annealing, respectively.

It is generally established that the strain shifts the paraferroelectric phase transition temperature.^{5,11,20} Our above Raman data also emphasize the effect of strain on T_C , clearly demonstrating the realization of RT ferroelectricity in STO thin films via strain engineering. Recently, Goncharova *et al.*¹⁷ and Amy *et al.*¹⁶ have reported how the elemental composition of the interface and how the epitaxial film itself change under annealing treatments. According to them, the STO/Si interface undergoes substantial changes with the process of strontium, titanium, or silicon atom diffusions and the formation of interfacial layers composed of SrO, SiO_2 , etc. As a result, the interfacial layers become crucial, since they act as if a “reconstructed” substrate when their composition and thickness change. As T_A is enhanced, the interfacial layers grow and combine, with the composition changing from “SrO and SiO_2 ” at 700 °C to “SrO, $TiSi_2$, and SiO_2 ” at 1000 °C, and experiencing “Sr–Si– O_x sandwiched between SrO and SiO_2 ” at 800 °C and “SrO, SiO_2 desorption, and Ti diffusion into the silicon bulk” at 900 °C.

Considering that the films were annealed at high temperatures in oxygen, defects such as oxygen vacancies are neglected. Therefore, strain may come from two parts, one is the lattice mismatch between the film and the interfacial layers or the substrate and the other is the thermal expansion mismatch between them. We concentrate on the latter, since the rotation of the STO layer with respect to the Si substrate by 45° mentioned above leads to a lattice mismatch relatively small at 1.7%,^{18,19,22} and annealing at high temperatures will further release this strain^{24,25} with the improvement of the film crystallinity.¹⁴ Another important reason is that above 550 °C annealing, there already exist the interfacial layers, the top of which is SrO, which contributes almost the same effects on the lattice mismatch strain under different annealing conditions above 550 °C.¹⁷

Based on the thermal expansion coefficients (TEC) of the interfacial layers and substrate at various T_A ,^{26–28} we can calculate the overall TEC value of the reconstructed substrate from the STO/Si interface composition. Thermally induced strain is then yielded via the difference in the TEC values between STO (α_{film}) and the reconstructed substrate (α_{sub}):¹³ $\epsilon_{thermal} = \int_{T_1}^{T_2} (\alpha_{sub} - \alpha_{film}) dT$. As shown in Fig. 3, it is found that the thermally induced strain is tensile for 700 °C annealing (0.42%) and 800 °C (0.34%), and compressive for 900 °C (–0.07%) and 1000 °C (–0.38%). From Fig. 3, T_C enhances as the magnitude of the in-plane compressive strain increases. The tremendous change in strain from 800 to 900 °C annealing demonstrates an onset of titanium into the silicon bulk ($TiSi_2$ can be formed), thus the continuity of the STO film is broken.¹⁷ It should be noted that 900 °C annealing gives the smallest thermal strain, indicating the best crystallinity,^{18,29} consistent with the results shown in Fig. 1(a), where the Raman spectrum of 900 °C T_A sample displays the weakest Raman intensity.

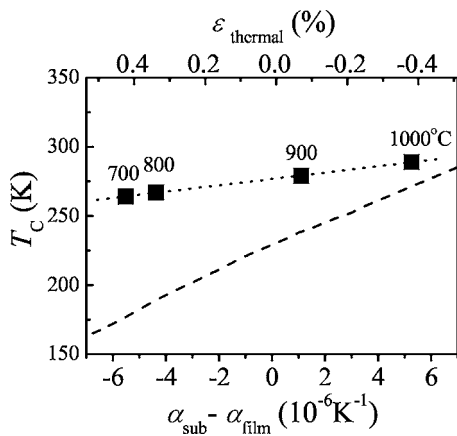


FIG. 3. Dependence of T_C on the thermal expansion coefficient mismatch and thermal strain determined from the TO_4 hard mode Raman intensities of different T_A . The dotted curve displays a linear fit to the thermal strain dependence, the dashed one demonstrates the predicted behavior of T_C (Ref. 30).

In Fig. 3, the dotted curve is a linear fit to the results, while the dashed curve shows the predicted behavior of T_C by Pertsev *et al.*³⁰ The deviation can be explained as a temperature broadening of paraferroelectric phase transition in STO thin films.¹⁰ Since the TO_4 mode Raman intensity is related to the atomic displacement or polarization,²⁰ it reflects the volume in the ferroelectric phase. When the temperature increases, ferroelectric regions reduce while paraelectric ones expand, instead of disappearing or occurring at a well-defined point.²¹ Tikhomirov *et al.*³¹ have shown by scanning optical microscopy that local ferroelectric and paraelectric regions coexist over a broad temperature range. Furthermore, the experimental and theoretical curves approach with each other as T_A increases, indicating that annealing would relax the inhomogeneous strain which is one of the causes for broad ferroelectric phase transition in films caused by the defects.¹¹

Figure 4 illustrates that the frequency of TO_4 phonon shifts downward from $\sim 550 \text{ cm}^{-1}$ to less than 540 cm^{-1} with increasing temperature, and for the higher T_A , the lower the frequency of TO_4 near RT. We suggest that this phenomenon can also be regarded as a sign of the process of the paraferroelectric phase transition, as shown by the dash-dotted lines in Fig. 4.

This work was supported by the National Natural Science Foundation of China (Contract Nos. 10734020 and 10674094), the National Major Basic Research Project 2006CB921507, the Minister of Education of PCSIRT (Con-

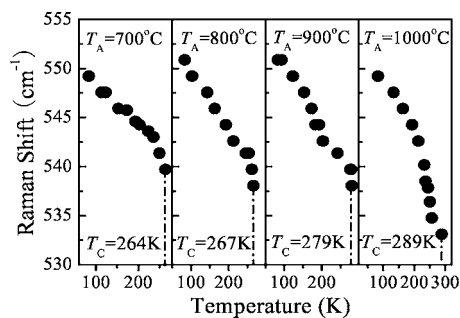


FIG. 4. Raman frequency of the TO_4 hard mode in STO thin films with different T_A as a function of temperature. The dash-dotted lines show points where this mode vanishes.

tract No. IRT0524), and the Shanghai Municipal Commission of Science and Technology Project 05QMH1411 and 06JC14039. The authors would like to acknowledge Professor R. Liu at Fudan University for providing the samples.

¹R. Waser and D. M. Smyth, in *Ferroelectric Thin Films: Synthesis and Basic Properties*, edited by C. P. de Araujo, J. F. Scott, and G. W. Taylor (Gordon and Breach, Amsterdam, 1996), p. 47.

²M. Nishitsuji, A. Tamura, T. Kunihisa, K. Yahatu, M. Shibuya, M. Kitagawa, and T. Hirao, *IEEE GaAs Integrated Circuit Symposium* (IEEE, New York, 1993), p. 324.

³R. Droopad, Z. Y. Yu, J. Ramdani, L. Hilt, J. Curless, C. Overgaard, J. L. Edwards, J. Finder, K. Eisenbeiser, J. Wang, V. Kaushik, B. Y. Ngyuen, and B. Ooms, *J. Cryst. Growth* **227**, 936 (2001).

⁴S. Gupta and R. S. Katiyar, *J. Raman Spectrosc.* **32**, 885 (2001).

⁵J. H. Haeni, P. Irvin, W. Chang, R. Uecker, P. Reiche, Y. L. Li, S. Choudhury, W. Tian, M. E. Hawley, B. Craigo, A. K. Tagantsev, X. Q. Pan, S. K. Streiffer, L. Q. Chen, S. W. Kirchoefer, J. Levy, and D. G. Schlom, *Nature (London)* **430**, 758 (2004).

⁶H. Wu and W. Z. Shen, *Phys. Rev. B* **73**, 094115 (2006).

⁷D. A. Tenne, A. Soukiassian, X. X. Xi, H. Choosuan, R. Guo, and A. S. Bhalla, *Phys. Rev. B* **70**, 174302 (2004).

⁸H. Taniguchi, T. Yagi, M. Takesada, and M. Itoh, *Phys. Rev. B* **72**, 064111 (2005).

⁹H. Taniguchi, M. Takesada, M. Itoh, and T. Yagi, *Ferroelectrics* **337**, 1303 (2006).

¹⁰D. A. Tenne, A. Soukiassian, X. X. Xi, T. R. Taylor, P. J. Hansen, J. S. Speck, and R. A. York, *Appl. Phys. Lett.* **85**, 4124 (2004).

¹¹D. A. Tenne, A. M. Clark, A. R. James, K. Chen, and X. X. Xi, *Appl. Phys. Lett.* **79**, 3836 (2001).

¹²K. J. Choi, M. Biegalski, Y. L. Li, A. Sharan, J. Schubert, R. Uecker, P. Reiche, Y. B. Chen, X. Q. Pan, V. Gopalan, L. Q. Chen, D. G. Schlom, and C. B. Eom, *Science* **306**, 1005 (2004).

¹³T. R. Taylor, P. J. Hansen, B. Acikel, N. Pervez, R. A. York, S. K. Streiffer, and J. S. Speck, *Appl. Phys. Lett.* **80**, 1978 (2002).

¹⁴D. H. Bao, N. Mizutani, X. Yao, and L. Y. Zhang, *Appl. Phys. Lett.* **77**, 1041 (2000).

¹⁵A. Y. Mao, K. A. Son, D. A. Hess, L. A. Brown, J. M. White, D. L. Kwong, D. A. Roberts, and R. N. Vrtis, *Thin Solid Films* **349**, 230 (1999).

¹⁶F. Amy, A. S. Wan, A. Kahn, F. J. Walker, and R. A. McKee, *J. Appl. Phys.* **96**, 1601 (2004); *J. Appl. Phys.* **96**, 1635 (2004).

¹⁷L. V. Goncharova, D. G. Starodub, E. Garfunkel, T. Gustafsson, V. Vaithyanathan, J. Lettieri, and D. G. Schlom, *J. Appl. Phys.* **100**, 014912 (2006).

¹⁸L. Hilt Tinsinger, R. Liu, J. Kulik, X. Zhang, J. Ramdani, and A. A. Demkov, *J. Vac. Sci. Technol. B* **21**, 53 (2003).

¹⁹Z. Yu, J. Ramdani, J. A. Curless, C. D. Overgaard, J. M. Finder, R. Droopad, K. W. Eisenbeiser, J. A. Hallmark, W. J. Ooms, and V. S. Kanchik, *J. Vac. Sci. Technol. B* **18**, 2139 (2000).

²⁰D. A. Tenne, A. Bruchhausen, N. D. Lanzillotti-Kimura, A. Fainstein, R. S. Katiyar, A. Cantarero, A. Soukiassian, V. Vaithyanathan, J. H. Haeni, W. Tian, D. G. Schlom, K. J. Choi, D. M. Kim, C. B. Eom, H. P. Sun, X. Q. Pan, Y. L. Li, L. Q. Chen, Q. X. Jia, S. M. Nakhmanson, K. M. Rabe, and X. X. Xi, *Science* **313**, 1614 (2006).

²¹Y. L. Du, G. Chen, and M. S. Zhang, *Solid State Commun.* **130**, 577 (2004).

²²F. S. Aguirre-Tostado, A. Herrera-Gómez, J. C. Woicik, R. Droopad, Z. Yu, D. G. Schlom, J. Karapetrova, P. Zschack, and P. Pianetta, *J. Vac. Sci. Technol. A* **22**, 1356 (2004).

²³T. Ostapchuk, J. Petzelt, V. Železný, A. Pashkin, J. Pokorný, I. Drbohlav, R. Kužel, D. Rafaja, B. P. Gorshunov, M. Dressel, Ch. Ohly, S. Hoffmann-Eifert, and R. Waser, *Phys. Rev. B* **66**, 235406 (2002).

²⁴J. S. Horwitz, W. Chang, W. Kim, S. B. Qadri, J. M. Pond, S. W. Kirchoefer, and D. B. Chrisey, *J. Electroceram.* **4**, 357 (2000).

²⁵D. Su, T. Yamada, V. O. Sherman, A. K. Tagantsev, P. Murali, and N. Setter, *J. Appl. Phys.* **101**, 064102 (2007).

²⁶A. D. Bruce and R. A. Cowley, *J. Phys. C* **6**, 2422 (1973).

²⁷R. J. Beals and R. L. Cook, *J. Am. Ceram. Soc.* **40**, 279 (1957).

²⁸A. M. Ardila, O. Martínez, M. Avella, J. Jiménez, B. Gérard, J. Napierala, and E. Gil-Lafon, *J. Appl. Phys.* **91**, 5045 (2002).

²⁹S. Myhajlenko, A. Bell, F. Ponce, J. L. Edwards, Jr, Y. Wei, B. Craigo, D. Convey, H. Li, R. Liu, and J. Kulik, *J. Appl. Phys.* **97**, 014101 (2005).

³⁰N. A. Pertsev, A. G. Zembilgotov, S. Hoffmann, R. Waser, and A. K. Tagantsev, *J. Appl. Phys.* **85**, 1698 (1999).

³¹O. Tikhomirov, H. Jiang, and J. Levy, *Appl. Phys. Lett.* **77**, 2048 (2000); *Phys. Rev. Lett.* **89**, 147601 (2002).